

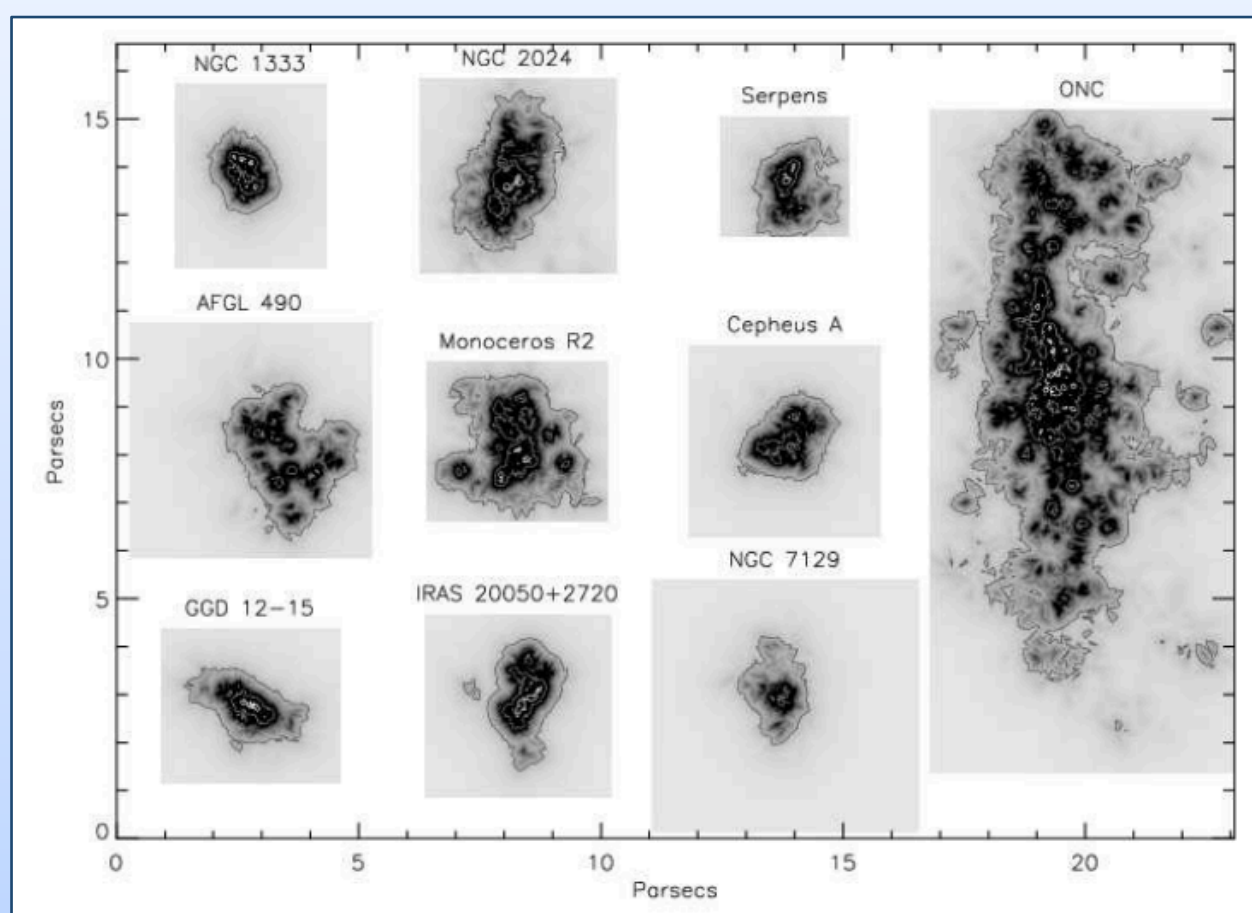
L. Venuti¹, L. Prisinzano¹, G. Sacco², E. Flaccomio¹, R. Bonito¹, F. Damiani¹, G. Micela¹, M. Guarcello¹,
GES and CSI2264 Collaborations (<https://www.gaia-eso.eu/>; <http://csi2264.ipac.caltech.edu/>)



¹ INAF – Osservatorio Astronomico di Palermo; ² INAF – Osservatorio Astrofisico di Arcetri

Corresponding author: Laura Venuti (lvenuti@astropa.unipa.it)

1. Times and modes of star cluster formation



Distribution of infrared excess sources in ten star clusters surveyed with Spitzer (Allen et al. 2007).

Large scale surveys of young clusters in different environments revealed:

- complex and varying morphologies (compact/spherical vs. elongated)
- hierarchic and filamentary structure, multiple subclusterings
- spatially and kinematically distinct subpopulations

Cluster formation: monolithic collapse or sequential process?

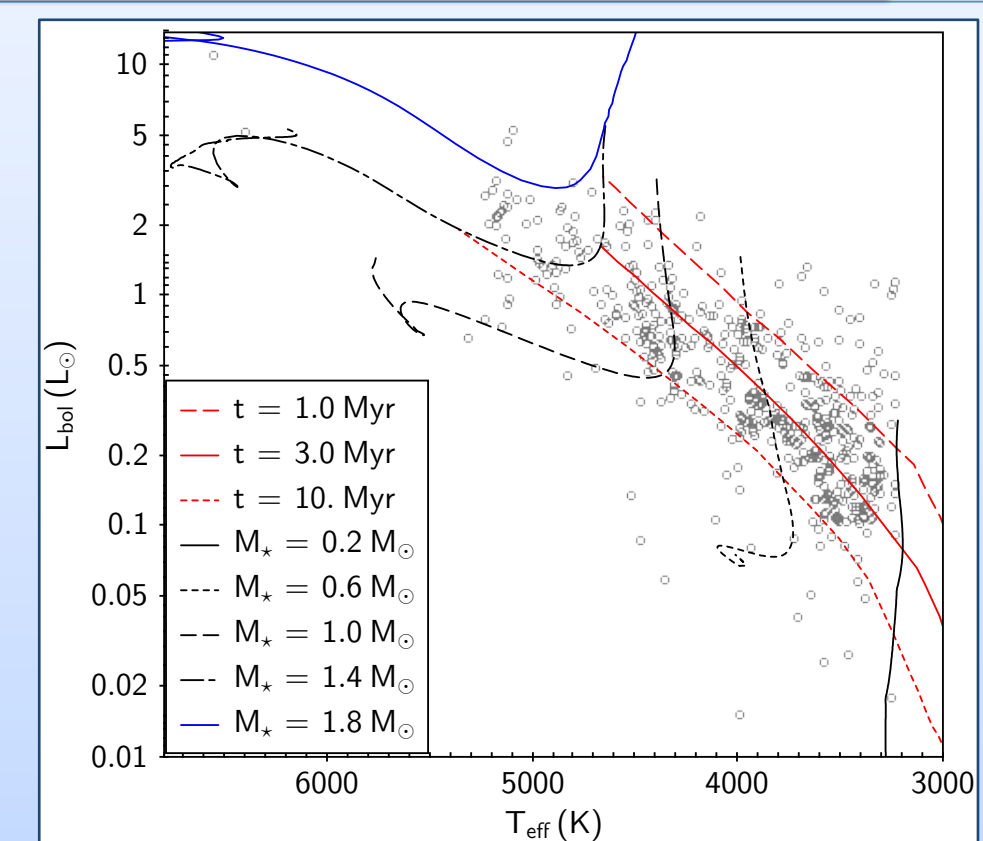
2. The interest of age spreads in young clusters

The *intra-cluster age dispersion* bears information on the duration of star formation activity within the region:

- *single, short-lived formation burst*
→ *coeval cluster members*
- *sequential, prolonged process*
→ *age spread among members*

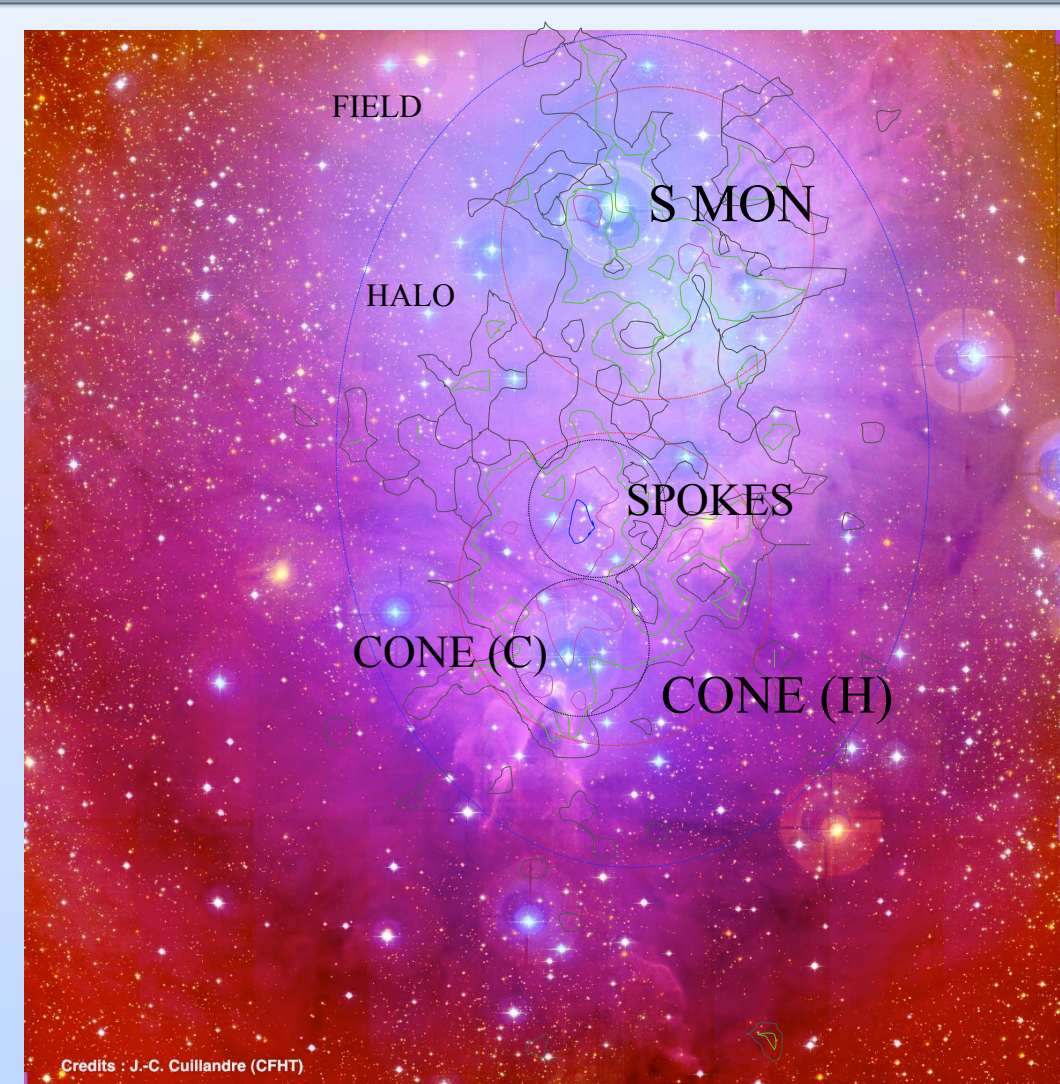
Individual stellar ages can be estimated from *isochrone-fitting* on the *HR diagram*.

Caveat: observational uncertainties (e.g., Hartmann 2001, Soderblom 2010, Jeffries et al. 2011)



HR diagram for NGC 2264 (Venuti et al., submitted; isochrones from Baraffe et al. 2015). The vertical spread at any T_{eff} appears indicative of a 10 Myr age spread.

3. NGC 2264: basic information



CFHT *u,g,r* color picture of NGC 2264 with surface density levels of H α emission stars and cluster subregions from Sung et al. (2008, 2009).

- **Distance:** 760 parsecs
- **Average age:** 3 Myr
- **Average A_V :** 0.4 mag
- **Population:** > 1000 members
- **Disk fraction:** ~50%

➤ Evidence of **multiple subclusterings** from the distribution of Class I/II/III members across the region (e.g., Sung et al. 2009)

➤ **Complex kinematic structure** with distinct subpopulations

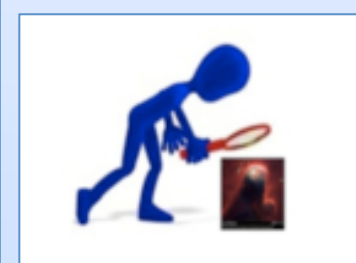
(Fűrész et al. 2006; Tobin et al. 2015; Sacco et al., in prep.)

4. NGC 2264: observations and sample selection



Gaia-ESO Survey [Gilmore et al. 2012; Randich et al. 2013]

- VLT/FLAMES spectra for 1892 targets in the NGC 2264 field
- Stellar T_{eff} ; youth (Li), accretion (H α) and gravity indicators

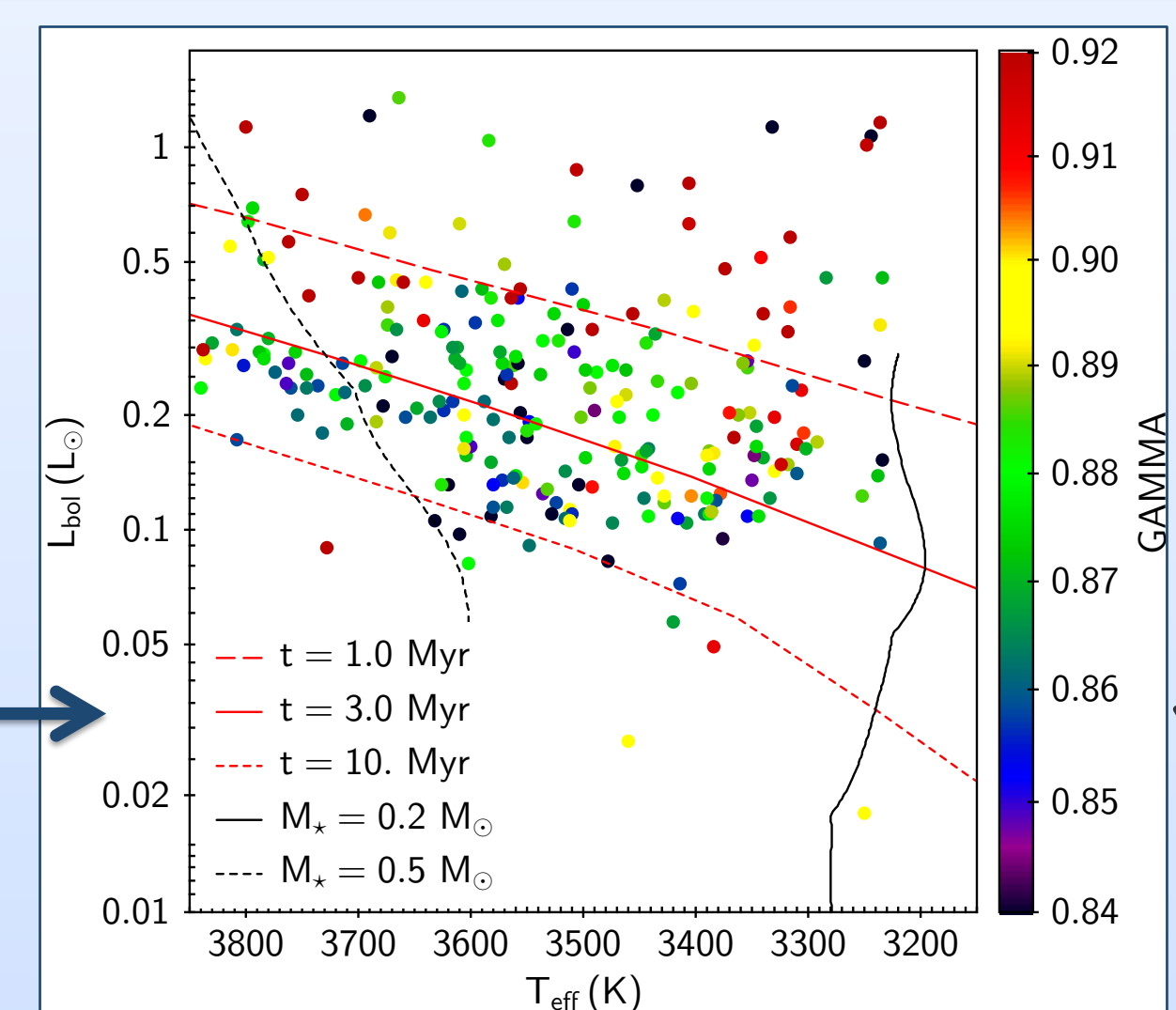


Coordinated Synoptic Investigation of NGC 2264 [Cody et al. 2014]

- X-rays to IR time series photometry (Chandra, CFHT, *CoRoT*, *Spitzer*)
- Accretion (UV excess) and disk (IR excess) diagnostics

- ✓ **655 cluster members** common to the two surveys (Li absorption, H α emission, UV/IR excess, X-ray emission, variability)
- ✓ M_* of objects in the sample range from 0.2 to 1.8 M_{\odot}
- ✓ 30% **disk-bearing** objects, 58% **disk-free** objects
- ✓ 29% **accreting** objects, 62% **non-accreting** objects

5. Intrinsic age spread in NGC 2264

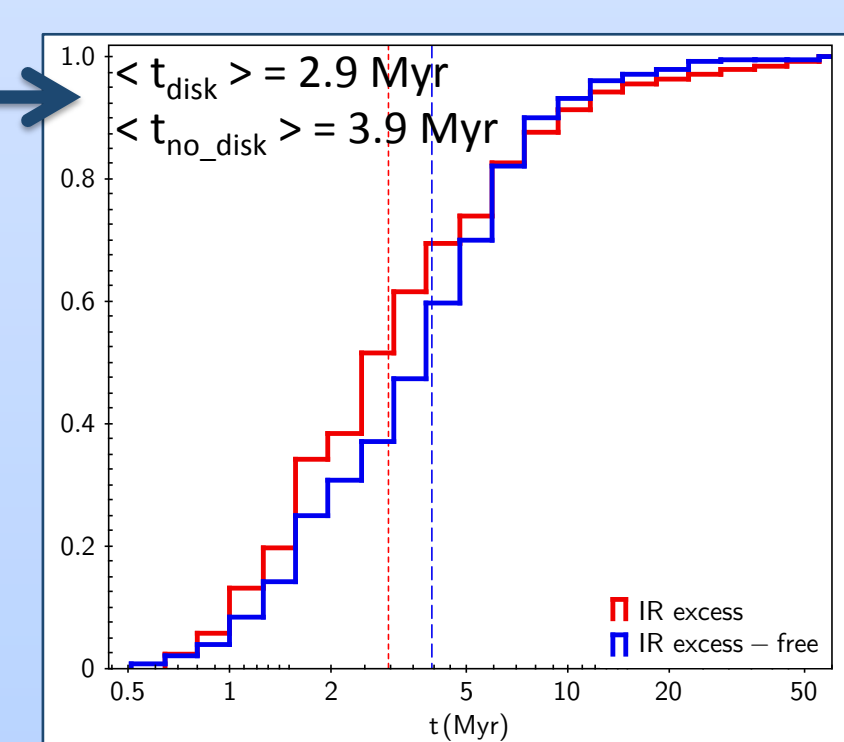


HR diagram for M-type stars in NGC 2264 (model tracks from Baraffe et al. 2015). Colors are scaled following the GES γ -index (Damiani et al. 2014), a spectroscopic index sensitive to stellar gravity and an empirical age indicator independent of photometric age.

- GES T_{eff} + *g,r,i* photometry (CFHT) → **individual A_V** (cf. Covey et al. 2007)
- *i*-band + BC_i (Girardi et al. 2008) → L_{bol}
- Robust approach to derive L_{bol} that reduces uncertainties due to differential reddening, veiling and disks
- Typical $\text{err}_{L_{\text{bol}}}/L_{\text{bol}} \sim 0.13$

➤ HR diagram exhibits **significant spread in L_{bol}** at any T_{eff}

➤ Model isochrones suggest: $\langle t_{\text{NGC2264}} \rangle = 3.6 \text{ Myr}$
rms dispersion = 0.35 dex

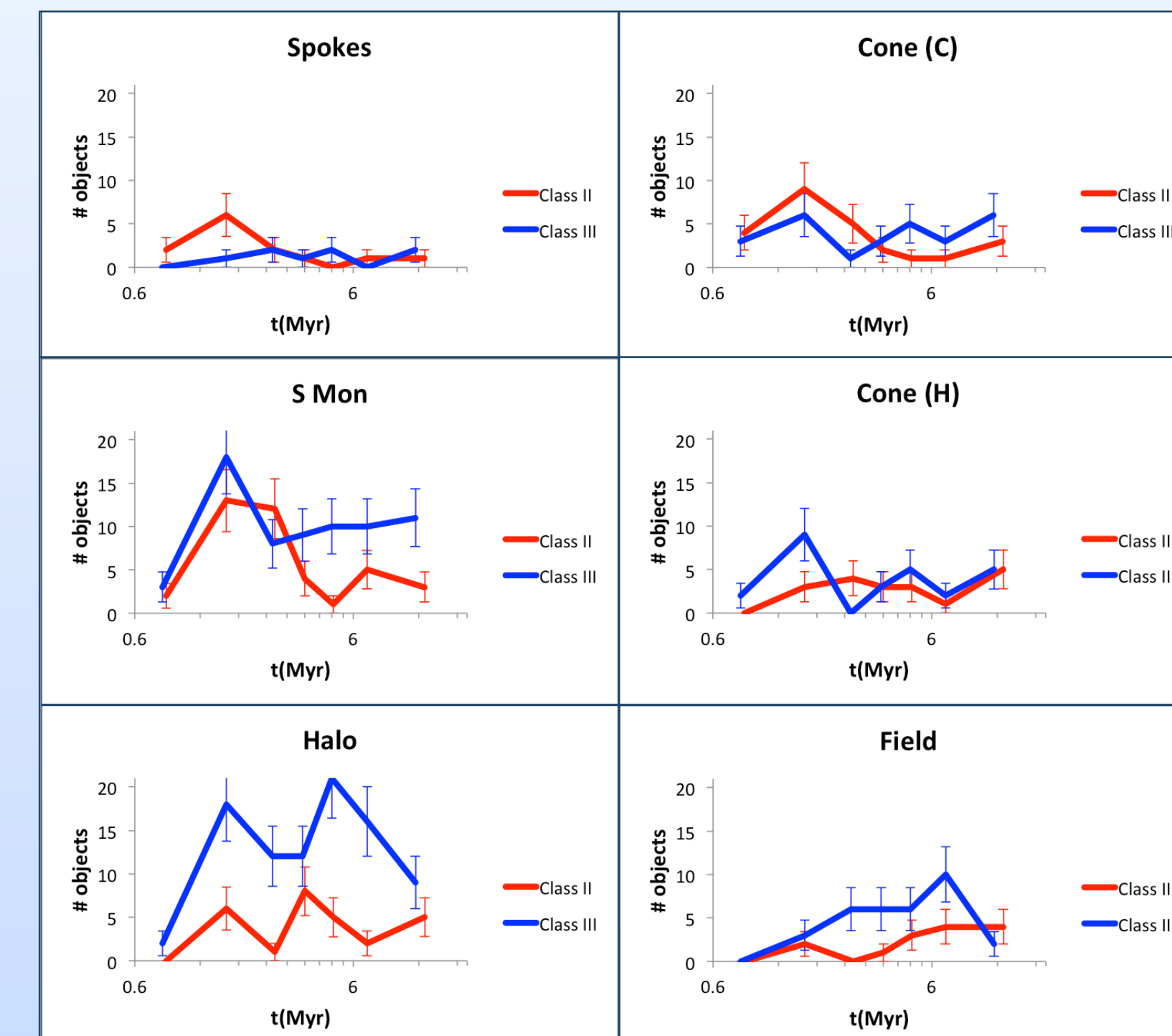


Cumulative distributions in isochronal age for disk-bearing (Class II, red) and disk-free (Class III, blue) cluster members.

Correlations with observable stellar properties support a real age spread:

- ✦ stars still **possessing a disk** appear **younger** than stars without disks
- ✦ **1–3 Myr** stars are associated with **lower gravities** than 3–10 Myr stars (two-sample K-S p -value = 0.004)

6. Cluster structure and star formation history



Number of objects and disk fraction across NGC 2264.

Region	Tot #	Class II (%)
Spokes	44	47.7 ^{+18.2}
Cone (C)	80	41.3 ^{+12.5}
Cone (H)	70	28.6 ^{+14.3}
S Mon	195	31.3 ^{+11.8}
Halo	175	20.6 ^{+10.9}
Field	91	28.6 ^{+12.1}

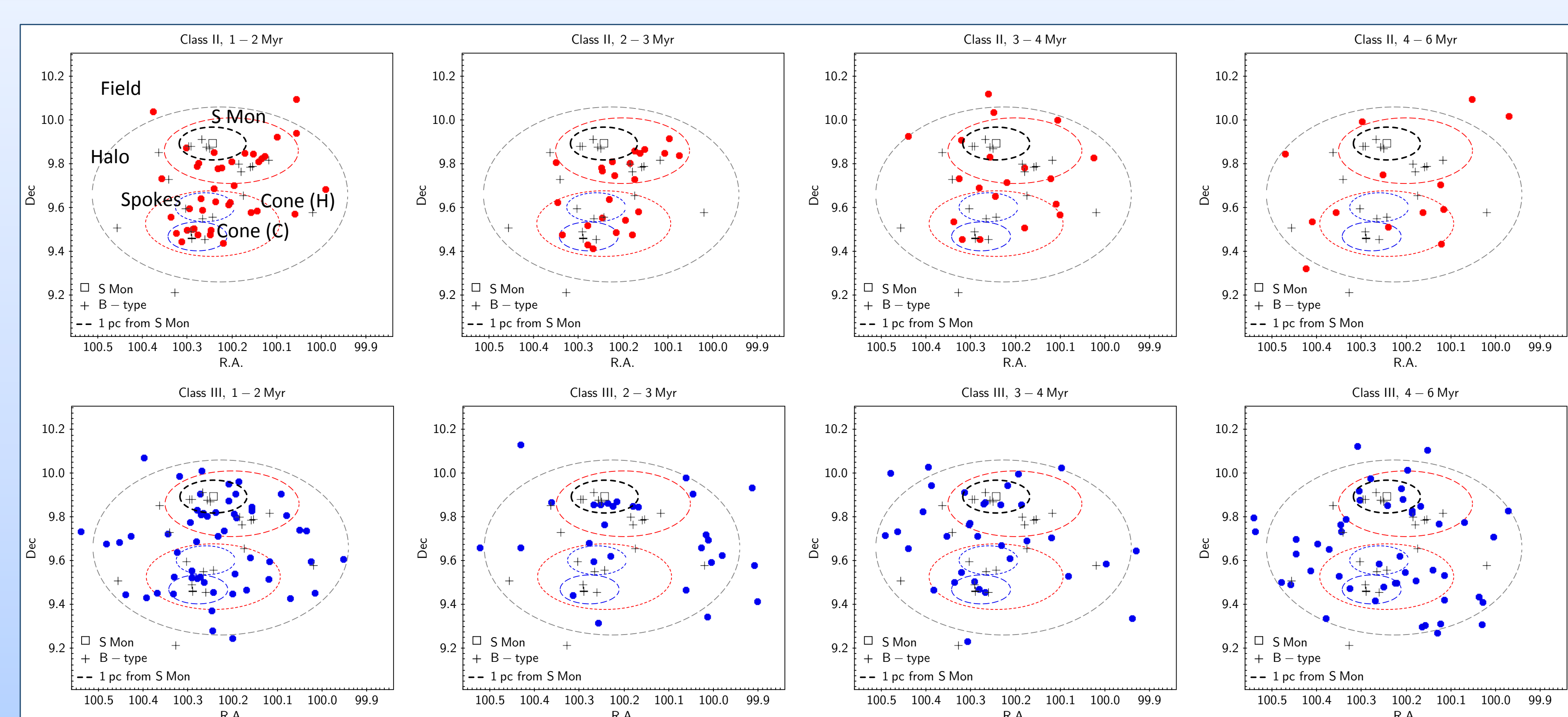
Median age of Class II/Class III sources across the cluster.

	Class II Myr	Class III Myr
Spokes	1.71 ^{-0.05}	4.39 ^{-1.08}
Cone (C)	1.91 ^{-0.06}	4.13 ^{-0.49}
Cone (H)	3.96	3.45 ^{+0.22}
S Mon	2.65 ^{-0.20}	3.72 ^{+0.03}
Halo	3.85	4.16 ^{+0.08}
Field	6.43	4.60 ^{+0.13}

Number of disked (red) and non-disked (blue) objects, as a function of age, in each of the six subregions shown in the second left panel.

- ✦ The **northern** (S Mon) and **outer** regions comprise **>60%** of members
- ✦ The **southern, central** regions (Spokes, Cone) have **highest disk fractions**
- ✦ **Class II** stars in **Spokes, Cone (C)** are on average **younger** than elsewhere
- ✦ The number of **Class II** stars in **S Mon** declines sharply at $t \geq 2.5 \text{ Myr}$, **qualitatively different from the trends observed in the other subregions**

7. Impact of environmental conditions on disk evolution



- Massive stars in NGC 2264: **one O-type** (binary S Mon) and **two dozen B-type**
- **Dearth of Class II sources close to S Mon** after the first couple of Myr
- **FUV flux** from S Mon can induce **photo-evaporation**; combined with **viscosity**, this may trigger **rapid disk dispersal**

Conclusions:

- ✓ Age spread of ~4 Myr within NGC 2264
- ✓ Multiple episodes of star formation
- ✓ Star formation began in the northern part of the cluster, and continues in the most embedded, southern regions
- ✓ Non-uniform environment conditions impact disk lifetimes across the cluster